A Multi-Track Elevator System for E-Commerce Fulfillment Centers

by

Rachel M. Hoffman

B.S., University of Florida (2015)

Submitted to the Department of Mechanical Engineering
in partial fulfillment of the requirements for the degree of

Master of Science in Mechanical Engineering

at the

MASSACHUSETTS INSTITUTE OF TECHNOLOGY

June 2017

Author ..... Signature redacted
Department of Mechanical Engineering
May 18, 2017

Certified by ..... Signature redacted
H. Harry Asada
Ford Professor of Engineering
Thesis Supervisor

Accepted by ..... Signature redacted
Rohan Abeyaratne
Quentin Berg Professor of Mechanics
Graduate Officer

A Multi-Track Elevator System for E-Commerce Fulfillment Centers

by

Rachel M. Hoffman

Submitted to the Department of Mechanical Engineering
on May 18, 2017, in partial fulfillment of the
requirements for the degree of
Master of Science in Mechanical Engineering

Abstract

Fulfillment centers located in densely populated urban areas are an ever-growing need for leading online consumer websites. These urban fulfillment centers have limited land mass and must have innovative solutions to transport goods within the available vertical space. This work presents a Multi-Track Elevator (MTE) System, a competitive solution for rapid access and retrieval of goods in high-rise e-commerce fulfillment centers and warehouses. The MTE System consists of multiple vertical rails connected with angular traverse rails that allow multiple carriages to go up and down without collision. A novel turning point system switches track routes so that several carriages can move across the multiple rails for rapidly accessing many floors and collecting diverse goods. Unlike existing vertical-horizontal grid elevators and rail systems, the roller-coaster type, self-powered carriages on the MTE system do not have to stop at switching points, but can continually move across the network of rails. Further, this work describes the architecture of the rail network system and techniques for switching multiple rails, followed by the design of vertical turntables for smooth, continuous rail switching. Finally, outlining the use of a simple route optimization algorithm, diverse elevator systems are compared with respect to total traveling time and distance. A proof-of-concept prototype has been built and is presented.

Thesis Supervisor: H. Harry Asada
Title: Ford Professor of Engineering

Acknowledgments

I would like to thank my mother, father, and brother, for their endless support and love. Your guidance has shaped me into the person I am and I hope to make you proud of not only my academic and professional success, but also my character. I am a direct reflection of your love and kindness, and I hope to continue shining bright. I love you bigger than the whole moon, the whole stars, the whole everything, and nothing will ever change that.

I would like to thank Jason Bice for his constant encouragement and patience throughout my time as a graduate student. Although we are living apart, I feel closer to you than ever. You have helped me grow as a person and as an engineer and I treasure every moment shared with you. You are an limitless source of warmth and laughter and I love all of our inside jokes and all of our shared dreams and goals.

I would like to thank all of my aunts, uncles and cousins for their support, love and for being my personal cheering squad during my entire academic career.

I would like to thank my fantastic labmates in the d'Arbeloff Lab, for being some of the most inspiring, patient, intelligent and fun people I have ever had the pleasure of working with.

Contents

List of Figures

Chapter 1

Introduction

Rapid growth of the e-commerce industry has required competition between industry leaders to provide the quickest response from the moment the customer makes an online purchase, to the moment the purchase arrives at their doorstep. Currently, many e-commerce companies require large warehouses to store, package and distribute their products. These companies are facing a major technological challenge when attempting to make speedy deliveries to the center of densely populated metropolitan areas [6]. One way e-commerce companies can reduce delivery times to these areas is by locating distribution warehouses as close to the city center as possible. However, due to space limitations, in order to maintain high levels of productivity online retailers will have to take advantage of technology that can change the layout of fulfillment centers from large floor foot prints to ones with smaller footprints and increased vertical space [6].

1.1 Background and Motivation: Warehouse Automation

Since the 1950s, vertical stacking and handling of materials and products has been automated with Automatic Storage and Retrieval Systems (AS/RS) consisting of aisle captive storage cranes, handling unit-loads or mini-loads (typically, pallets or bins)

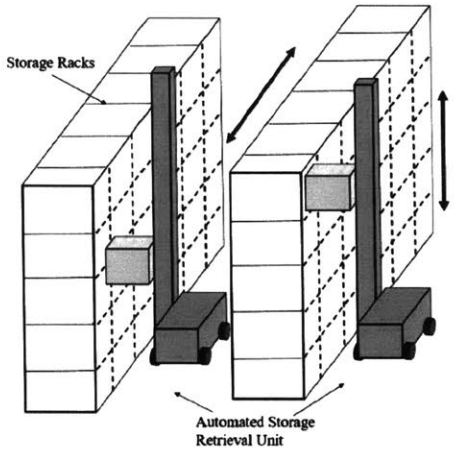

Figure 1-1: An example of an Automated Storage and Retrieval System

on shelving units in warehouses [11]. To meet the increasing demand of smaller orders with large product variety, the Autonomous Vehicle Storage and Retrieval System, AVS/RS, was developed. The AVS/RS consists of vehicles moving horizontally along rails within the storage racks and using lifts mounted along the rack periphery to provide the vertical movement[10]. Although the AVS/RS system provides flexibility in terms of vehicle and lift allocation, it requires longer flow paths from sequential vertical and horizontal travel as well as waiting times for vehicle use of lifts [12].

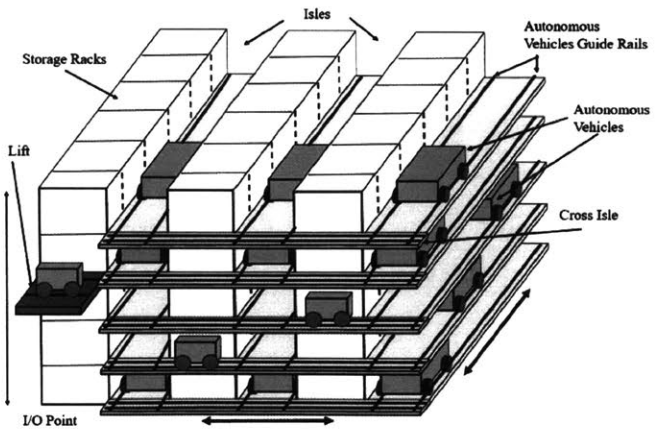

Figure 1-2: An example of an Autonomous Vehicle Storage and Retrieval System

Shuttle-based storage and retrieval systems (SBS/RS) were developed in an attempt to improve upon the operating capacity of the AVS/RS. In this system, two lifts capable of vertical movement of loads share a single mast to transport loads

from horizontally operating shuttles to the I/O point and vice versa. Hence, the two lifts cannot pass each other, and as a result, the upper lift can only reach the Input/Output (I/O) point if the lower lift is positioned at one of the aisles below the I/O point [5]. Another advanced product sorting and handling technology used

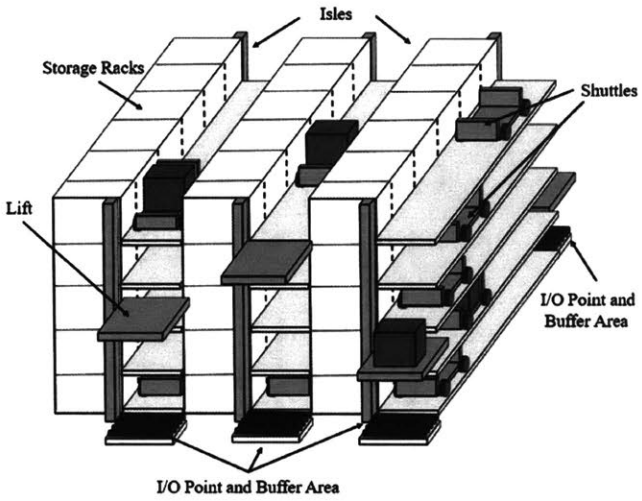

Figure 1-3: An example an Shuttle Based Storage and Retrieval System

by multiple companies is the Kiva Mobile Fullfullment System (MFS), now known as Amazon Robotics. The Kiva MFS is a network of robots that are controlled by software agents that interact with each robot on a warehouse management server and on computers at human operated product picking and packing stations [15]. Amazon Robotics may be useful, but the weight and height restrictions of the shelves make this technology only a partial solution to efficiency limitations for e-commerce in cities [14].

The elevator industry has been exploring advanced architectures that could potentially be adapted for use in warehouses. One architecture of interest is a type of circular motion elevator system that consists of multiple carriages operating in a loop, similar to a metro system. This system is able to potentially increase the shaft transport capacity by up to 50 percent and can increase a buildings usable area by up to 25 percent [1]. Although the Circular Motion Elevator (CME) system provides greater efficiency than a standard elevator, the circular motion of the carriages limits where each carriage can travel and requires carriages to follow a constrained timeline.

Thus, limiting the independence of each carriage to execute tasks.

1.2 Contributions and Overview

This thesis presents a Multi-Track Elevator (MTE) system, shown in Fig. 1-4, consisting of a network of multiple tracks and self-powered carriages that can move in the vertical direction and have flexibility in horizontal movement. The carriages are designed to move along a gridded rail system, and change directions at rail intersections using vertical turntables. This system is designed to be a significantly more efficient alternative to existing systems used in warehouses.

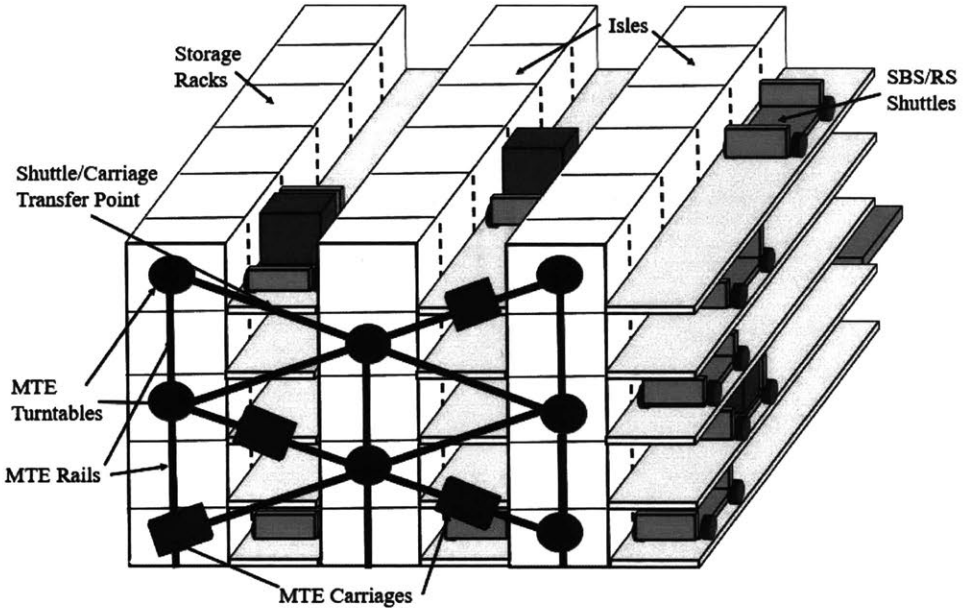

Figure 1-4: An example of the implementation of the MTE system with existing warehouse automation technology

Chapter 2 explores several rail grid architectures for adaptation into the MTE system as well as the functional requirements of the mechanism by which the MTE carriages smoothly transition from one rail section to the next.

In Chapter 3, the control scheme of the MTE System and the carriages. The low-level control by which the MTE turntables and the carriages communicate and signal the appropriate changes required for direction changes is discussed. The high-level

control consists of a simple form of path coordination between the carriages so that they may reach their target destination in the global optimal time.

Chapter 4 discusses the detailed design and implementation of the prototype Multi-Track Elevator System, including the rail network, turntables and carriages. The functional requirements of the MTE System are stated, and analyses are performed in order to specify and design the structure and actuation to meet these functional requirements. Furthermore, the complete manufacturing process and assembly of the MTE System is detailed.

Chapter 5 discusses the experimental validation of the MTE system through comparison with elevator architectures currently implemented in industrial warehouse settings as well as in high-rise buildings. Further validation is performed by discussing several scenarios in which the architecture of the MTE system is advantageous as well as a comparison between optimizing for the total system time traveled by all of the carriages and optimizing for the shortest path distance traveled by each carriage.

Chapter 6 provides a conclusion of the work done for this thesis, and recommendations for future work related to the Multi-Track Elevator System.

Chapter 2

Design Concept

2.1 Exploration of Rail Network Architectures

The two-dimensional grid structure, seen in Fig. 1-4, provides many potential path for multiple points, or in our case carriages, to travel between two nodes. Moving within a two-dimensional vertical wall, the square grid, seen in Fig. 2-1(a) allows each carriage to move in either vertical or horizontal directions. If oblique rails are added to the square grid, as depicted in Fig. 2-1(b), the net pass length moving from a grid node A to B will be shorter. In this grid structure four rails intersect at a grid node, and eight branches of rails exist at each node, giving eight choices of direction to proceed. This Octa-Grid structure creates more path opportunities, hence shorter passes moving to and from any given point on the wall. Fig. 2-1(c) depicts a grid architecture, where three rails intersect at each node. Horizontal rails have been eliminated in this design, which limits the directions of carriage movements from any one point to six choices. In this design, all the nodes are intersections of three rails except for the nodes at the wall boundaries.

By assuming that each block in the Square-Grid system in Fig. 2-1(a) is exactly one unit, the total distance traveled between arbitrary points A and B can be demonstrated. Using basic trigonometry, we can see that the total distance traveled for a carriage on the Square-Grid, Octa-Grid and Hexa-Grid architectures are 6 units, 4.24 units, and 4.6 units respectively. Although the traveling distances vary depending on

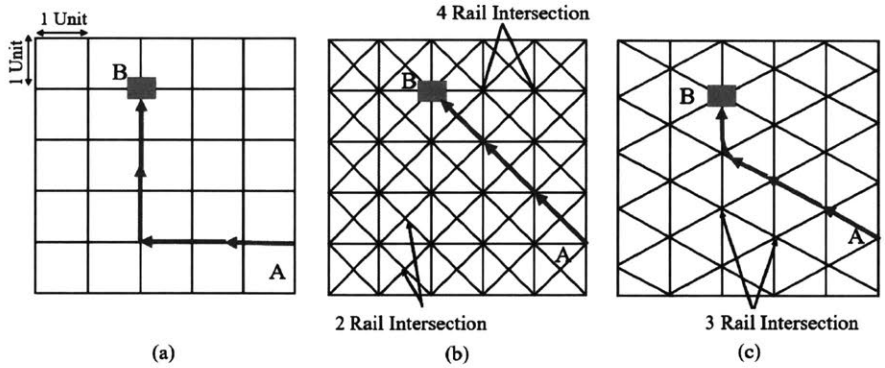

Figure 2-1: Grid architecture: (a) Square-Grid (b) Octa-Grid (c) Hexa-Grid

the start and end points, the Square-Grid requires the longest distance, followed by the Hex-Grid and the Octa-Grid architecture; $D_{Square} > D_{Hexa} > D_{Octa}$.

It can be concluded that, although the Octa-Grid structure provides the shortest distance traveled between any two points on the grid architecture, the increased complexity at the node-rail intersections provides additional manufacturing challenges. One of these challenges includes the need for increased size of the prototype to accommodate all of the rails. For example, it was determined that this system would be prototyped within my laboratory at approximately a 1/10th scale of current systems implemented in warehouses in order to effectively [9]

The Vertical Hexa-Grid architecture depicted in Fig. 2-1(c) provides the best compromise between length of distance traveled and ease of system manufacturing.

For applications where carriages will have to visit stations that are distributed horizontally, a horizontal Hexa-Grid architecture will be more effective than the Vertical Hexa-Grid architecture, due to the avoidance of unnecessary direction changes to traverse in the horizontal direction.

2.2 Rail Transition

One of the most critical technical challenges in the development of two-dimensional rail systems is the realization of smooth transitions across multiple tracks and the steering of carriages at nodes where multiple tracks intersect. An existing solution

is to switch two sets of grippers, one holding a horizontal rail and the other holds a vertical rail. A carriage approaching a node with one set of grippers holding a horizontal rail grasps a vertical rail at the intersection with another set of grippers, and then disengages the set of horizontal grippers. Such an approach requires a car to stop at an intersection for switching grippers, thereby taking a long time to cross over each intersection [1].

The inefficient discontinuous transition can be eliminated by applying a point switching technique. Similar to a railway turnout, a carriage can be guided from one branch of rails to another at an intersection. The wheel of a carriage is always engaged with some portion of the rail continually, and no discrete operation for engaging and disengaging grippers is involved. Unlike the traditional railway turnout that uses a pair of rail blades lying horizontally on the ground, this system is laid vertically. A turn table with multiple transition rails stands vertically and switches vertical rails.

Figure 2-2 presents the design concept for a Vertical Turnout Mechanism placed at the intersections of a grid rail system. The Mechanism consists of a Turntable, a set of Transition Rails, and an actuator (not shown in the Figure) that rotates the turntable. When a carriage approaches an intersection, the turntable rotates to connect the rails required for the incoming carriage's path. Figure 2-2 shows three transition rails secured to the turntable; a straight rail in the center, a left-curved rail, and a right-curved rail.

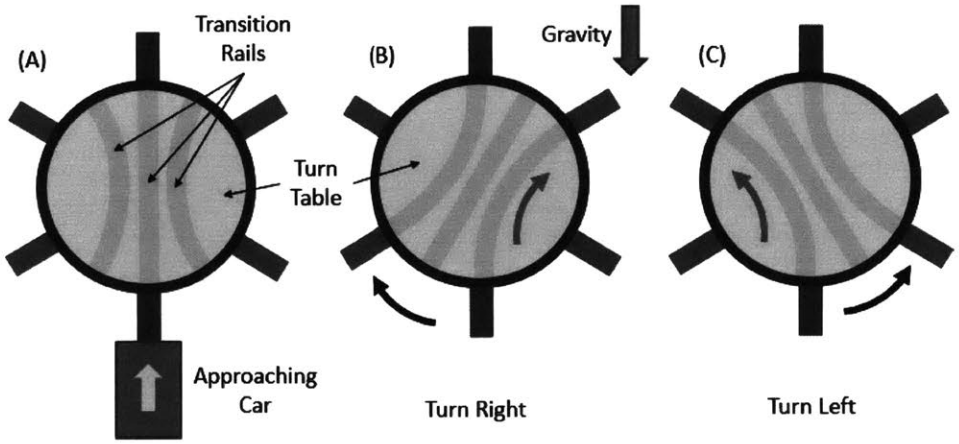

Figure 2-2: The design concept for a Vertical Turnout Mechanism

In case of moving straight, the turntable simply rotates to a specified angle, with the transition rail adopting the straight center configuration as seen in Fig. 2-2(A). When turning right or left, the positioning control of the turntable rotates to align one of the two curved rails to connect the rail of the incoming car to the desired outgoing rail as seen in Fig. 2-2(B) and 2-2(C), respectively. The carriage is continuously engaged with the connected rails, thus maintaining the traverse velocity. Although the three transition rails depicted in Fig. 2-2 allow only three available path directions, an arbitrary path across the entire two-dimensional grid is attainable by attaching the transition rails to a turntable with the ability to rotate 360°. By reducing the number of possible turn directions, the number of connections required by the turntable reduces drastically. The carriage needs to either continue straight or turn 120°. By having a single straight section and a single curved section, every possible rail combination is accounted for using a full 360° rotation. This turntable rail design can be seen in Fig 4-2.

Chapter 3

Control of the Multi-Track Elevator System

3.1 Low-Level Control

The central controller must be able to determine the location, direction and intended path of each carriage to appropriately control the carriages and turntables. In order to execute a turn, the central controller must know the exact moment the carriage begins and ends a turn, providing appropriate carriage motor commands that adapt to the differing arc lengths of the inner and outer curved rails of the turntable. The central controller must also be aware of the impending approach of a carriage to a turntable so that the appropriate turntable position can be assumed. Therefore, an indication mechanism, such as a Global Positioning Satellite (GPS) or Radio-frequency identification (RFID),must be implemented within the MTE system so the exact location of each carriage is known.

To implement the MTE system in areas where GPS technology is not be accurate enough to determine the unique, precise location of each carriage within a confined space, it was determined that the use of indication through the use of scanning or reading a particular code at a specific location would be the most feasible method of carriage tracking.

To facilitate localization of each carriage as well as turntable orientation com-

mands, each point used will need to be entirely unique. If the setup described previously is expanded to a larger system, such as the one depicted in Fig. 1-4 , a substantial number of unique points will be required. Methods such as using an Internal Position System (IPS) and RFID tags for autonomous mobile robot localization are currently implemented in many warehouses and are undergoing extensive research [16].

The locations required to place the tracking indicators, such as RFID tags, to facilitate successful operation of the carriages and turntables are the two points immediately on the intersection of the turntables and rails and the point located directly at the midpoint between the two turntables. As seen in Fig. 3-1, the former points will indicate the exact moment a carriage has begun traveling across the turning point mechanism and will allow for successful turning commands of the carriages. The latter will provide indication of a carriages approach to a turntable with sufficient advance notice to orient the turntable to the make the appropriate rail connections.

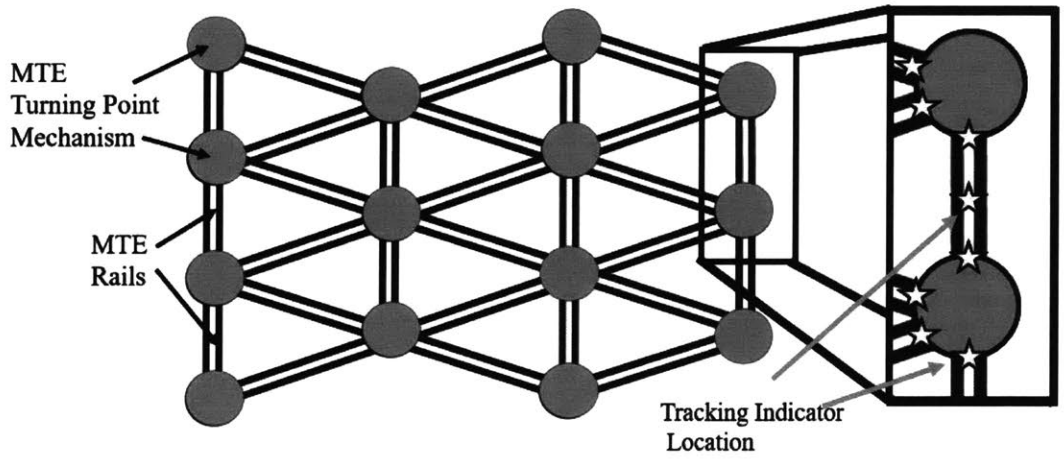

Figure 3-1: The locations of the tracking indicators to facilitate successful control of carriages and turntables within the Hexa-Grid rail structure

An affordable alternative to RFID tags that still allows for unique identification is using infrared (IR) LEDs configured to each output a unique signal. Using a single Mojo V3 FPGA Development Board, up to 84 IR LEDs can be controlled, more than

enough for the prototype depicted in Fig. 3-1. The IR LEDs are mounted to the inner section of the rails such that they are in-line with the top surface of the rails. To successfully read each IR LED, each carriage is equipped with IR Receiver.

3.2 High Level Control

Although the focus of this paper is on the design of the system, it was necessary for testing and validation to implement a basic form of distributed path planning of the carriages. The field of robot path planning has been extensively studied [8] and divided into two main categories, centralized planning and decoupled planning. Where centralized planning considers the various robots as separate components of a composite robot and decoupled planning creates a path for each robot independently of other robots and then considers interactions among the paths [8].

Due to the large dimension of the configuration space for complicated centralized planning problems, the time complexity is exponential in this direction, a decoupled path planning approach was chosen for implementing the MTE system. One approach to decoupled planning is known as path coordination. This approach generates a free path for each robot independently and then coordinates the paths to avoid collisions. To ensure robustness of a final solution, an additional algorithm based on a priority planning approach may be executed. Additional simplifications to the requirements of the path planning problem can be made when taking into account the path constraints due to the structure of the MTE system. These physical constraints allow the system to be represented as a graph with nodes with directionality constraints.

Although there are many well known graph searching shortest-path algorithms including Dijkstras algorithm [7], A* algorithm, and the Floyd-Warshall algorithm, the physical constraints placed on the system offer some serious challenges for successful implementation using a combination of path coordination and priority planning.

For example, say we have two carriages that require shortest paths to their respective targets, although all three algorithms will easily be able to calculate the shortest path of the first carriage, they may encounter some difficulties calculating

the shortest path of the second carriage that does not intersect the first carriage. It is not in the nature of these three algorithms to accept the a path that is not deemed the shortest to be the final solution. If say, carriage 2 had to extend its path to avoid carriage 1, then the three algorithms may run into a dead-end if they are prohibited from returning paths that avoid collisions.

To avoid this problem, it was determined that the simplest method to implement that would avoid collisions as well as provide the overall shortest allowed path for the carriages involved was to create a modified Depth-First-Search (DFS) algorithm [3] that utilizes known decoupled path planning methods. A standard DFS allows the search to travel as deep as possible from vertex to vertex before backtracking. This modified DFS algorithm explores all independent simple possible paths that multiple carriages can travel to reach target locations, and then chooses a final path based on collision avoidance in order of priority. The modified DFS algorithm determines an initial priority queue of the carriages and begins comparing the possible shortest paths of each carriage and eliminating conflicts based on priority. At any point, if the local minimum of the shortest possible path calculated for a particular priority queue matches the overall global minimum path length, the algorithm returns the shortest path for each of the carriages, as well as the turntables and LEDs projected to be encountered by each carriage as it traverses the system.

Although the distance between any two adjacent turntables is the same, it was determined that applying a weighting factor to increase or decrease the cost of traveling along certain rails should be applied to further optimize the system for a large number of carriages. An analysis was performed to determine the frequency at which a carriage would travel between any two nodes to reach any desired target node from any starting node. The results of this analysis can be seen in Fig. 3-2.

As seen in Fig. 3-2, the frequency of travel is divided into three categories, $freq \leq 11$, $11 < freq \leq 15$,$15 < freq$. The rails that will see the most potential traffic have a frequency of greater than 15 and the rails least likely to be used have a frequency of less than 11. A weighting factor ranging between 1 and 2 can be applied to the rails least likely to be traveled and the rails most likely to be traveled respectively.

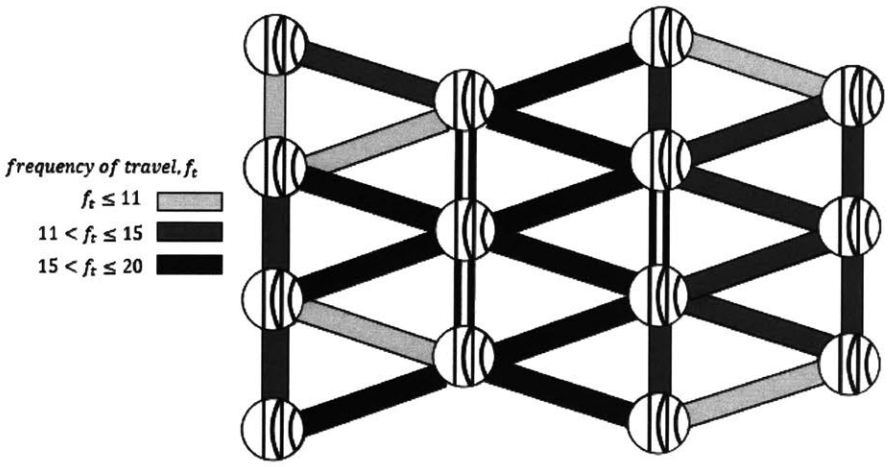

Figure 3-2: The frequency at which carriages executing the shortest path to another cross the rail segments warehouse automation technology

This variable weighting factor 'encourages' the system to make use of the rails least likely to be traveled in order to leave available space for the heavily-trafficked rails.

Chapter 4

Design Implementation

4.1 Turntable and Rail Design

The current dimensions of the unit loads carried by one particular SBS/RS system currently used in industry is a minimum of 150 mm x 200 mm x 80 mm and a maximum of 600 mm x 400 mm x 250 mm [9]. Based on the current schematic for this SBS/RS, we can approximate the size of the shuttle to be approximately 200 mm longer and wider than the maximum dimension of the unit load. Therefore we can approximate the maximum length and width of the shuttle used in industry to be 800 mm x 600 mm.

It was determined that in order to sufficiently test and demonstrate the effectiveness of the MTE system, a prototype would be required to contain at least 14 turntable nodes. By designing an arrangement of the turntable nodes such that there were at least 7 vertical layers nodes with each layer containing two turntables arranged to form the Hexa-Grid rail structure seen in Fig. 3-1.

To accommodate the requirement for an expansive Hexa-Grid rail structure, it was determined that the dimensions of the carriage and rail system would be derived from a scaled version of the shuttle used in industry [9]. To obtain a reasonable dimension for use in design and calculation of the MTE system parameters, it was determined that a 1:12.6 scale of the shuttle system used in industry. This scale yields a base width of 63.5mm (2.5in) for the rail system and MTE carriage, seen in Fig. 4-2.

Due to the requirement of the MTE carriages to travel vertically along the rail structure, it was determined modern roller coasters contained several structural elements similar to the requirements of the MTE system. Modern roller coasters are able to travel in many different orientations without fear of the roller coaster car separating from the rails.

In roller coasters commonly implemented, there are two main types of roller coaster rail support designs. Both designs consist of two rails on which the roller coaster rides. The typical wheel design on a roller coaster car consists of a set of running wheels and up-stop wheels that gripping the top and bottom of the rail respectively, so that the roller coaster car can travel upright as well as upside down without leaving the track. An additional set of side friction wheels are grip the sides of the rails so that the roller coaster car remains in the center of the rail. One prominent design choice roller coaster manufacturers make is how to mount the side friction wheels on roller coaster car such that they grip either the inside or the outside of the rail. This choice leads to one of the main differences in roller coaster rail structure design, and the difference which is deemed most relevant to the design of the MTE system, is the location of the supports for these rails. If the roller coaster car is designed with the side friction wheels gripping the outside of the rail, the support for the roller coaster rail structure can be located along the centerline of the rail without interfering with the motion of the roller coaster car. If the side-friction wheels are mounted such that they grip the inside of the rail structure, the support for the rail structure must be fixed to the outside of the rails, as seen in Fig. 4-1.

By analyzing the initial design concept for the MTE turntable seen in Fig. 4-2, it can be seen that the second form of roller coaster rail structure will not be feasible due to the overlay of the straight rail segment and the curved rail segment. Therefore, it was determined that modeling the MTE carriage after a roller coaster with side-friction wheels mounted to the outside of the rail would be best suited to the MTE system.

Due to the desired mounting location of the side-friction wheels, there needs to be sufficient space between the rails at the turntable intersection so that the carriage

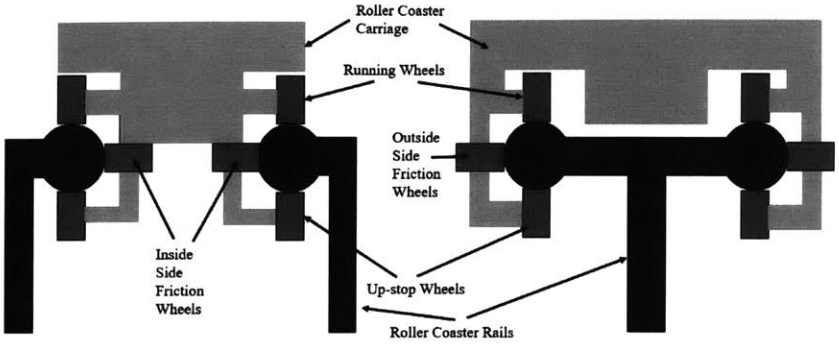

Figure 4-1: The two main designs of roller coaster carriages wheels and roller coaster rails

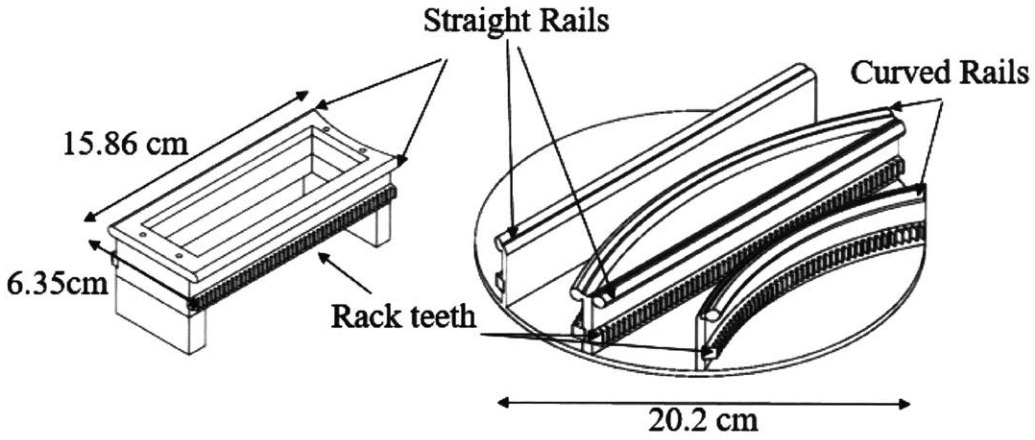

Figure 4-2: The design of the rail system and transition turntable platform

may travel without interfering with the adjoining rail sections as it enters and exits the turntable. The width of each rail section is equal to the base width of the rail section, 63.5 mm added to the diameter of the cylindrical rail itself, 6.35 mm. The circumference of the circle formed by six of these rail segments is found to be 380.1 mm.

It was estimated based upon the scaling of the MTE system that providing a clearance of approximately one inch on either side of a rail segment will allow for flexibility in the design of the carriage while ensuring that there would be no interference by the adjoint rail segments. Therefore, the diameter of the turntable was determined to be 203.2 mm (8 in).

A basic torque calculation was completed to determine the minimum torque re-

quired to rotate the turntable. The functional requirements of the MTE systems dictate that the carriage will never be traveling along the turntable while it is turning, therefore only the inertia of the turntable needs to be considered. To accommodate incoming carriages, the turntable should be able to perform a full rotation in a maximum of 2 seconds. Based on motor availability, an average speed of 30 RPM was selected for the motor calculation seen in (4.1).

$$\tau_{\text{motor}} = I\alpha = \frac{1}{2}(.345kg)(0.1016m)^2 \left(\frac{30rev}{1min} \frac{1min}{60sec} \frac{2\pi rad}{1rev} = \right) = 0.0056Nm \quad (4.1)$$

Integrated motors with a built-in controller (Dynamixel MX-106T and MX-64) were selected due to availability, ease of use, reduced cable requirement, and large torque outputs (8.4 Nm and 6 Nm respectively). These motors, while much stronger than required, allow for the scalability of the project, the addition of frictional forces due to tolerance errors and the implementation of additional methods to ensure precise positioning of the rails.

Due to the chosen operating mode of the Dynamixel motors preventing them from rotating continuously, the gear ratio for the gear attached to the turntable motor and the gear attached to the turntable was designed to be 1:1. This ratio ensures that a full rotation of the motor will result in a full rotation of the turntable. the hub of the Dynamixel motors are 28 mm in diameter and the width of the Dynamixel motors are 40 mm. In order to provide sufficient clearance for mounting the Dynamixels and Turntables on the wall, a pitch diameter of 50.8 mm (2 in) was chosen for the motor and turntable gears.

Each feasible rail position on the turntable requires a rotation of 30°. Common gear specifications were considered and compared to find a reasonable compromise between pitch and resolution. To have as precise of a resolution as possible, it was necessary to find the pitch that would provide the most gear teeth in the smallest amount of space. Based on gear availability, gears with a pitch of 32, a pressure angle of $14\frac{1}{2}^\circ$ and 62 teeth were selected. Although these gear teeth allow for an angular

resolution of 5.8°, the resolution of the Dynamixel motor is .088° which results in the precise positioning of the turntable.

To ensure the gears would not fail when the Dynamixel motor applied its continuously running torque,but would fail as a safety mechanism if the turntable became jammed, the following calculation was completed. We are able to solve for the maximum possible transmitted load before failure by rearranging the Lewis Factor Equation [4], where σ is the maximum bending tooth stress based on the ultimate tensile stress of the gear material, W_t is tangential tooth load, F the face width of the gear, Y is the Lewis form factor and DP is the diametral pitch.

$$W_t = \frac{\sigma FY}{DP} = \frac{\left(3.2 \times 10^7 \frac{N}{m^2}\right)(0.00635m)(.355)}{1365 \frac{teeth}{m}} = 54.5N \tag{4.2}$$

Therefore, to accommodate a factor of safety of 2, the maximum applied load that the gear teeth can handle is 27.25 N.

Using the maximum applied load, the maximum torque output from the motors that the gears can handle is calculated as follows.

$$\tau_{motor} = F_{transmitted}(r_{pitch}) = (27.25N)(.0254m) = 0.6921Nm \tag{4.3}$$

Based on the predicted maximum applied torque that can be applied to the turntable gears and the chosen gear parameters, the force causing the distance between the centers of the gears to spread can be calculated using the following equation.

$$F_{\text{spread}} = \frac{2\tau}{D_{pitch}} \tan(\phi) = \frac{2(0.6921Nm)}{.0508m} \tan(14.5°) = 7.033N \tag{4.4}$$

The manufacturer recommends that the motors use $\frac{1}{5}$ or less of the stall torque to create stable motions. Based on the previous calculation, the maximum torque that can be handled by the system is limited by the gear specifications, not the motors. As seen in the previous calculations, the gears attached to the turntable will successfully handle the applied torque from the recommended continuous motion of the Dynamixel motor, but will spread apart and begin skipping if the system becomes jammed or

encounters too much friction. This serves as a safety mechanism for the system to prevent damage to the motor and to the more complicated parts of the assembly.

One unique requirements of the turntable system is the precise positioning of the turntable when the rails on the turntable are required to align a particular rail combination on the MTE rail network. Although the Dynamixel motors provide a resolution .088°, the motor has an inherent backlash which can cause a misalignment error of up to 2.54 mm. Furthermore, the angular backlash. σ_a, between the gears transmitting torque from the motor to the turntable can be calculated as follows, using $r_1 = r_2 = r_{pitch}$, δ is a small amount to prevent gear jamming, ϕ is the pressure angle

$$\sigma_a = \frac{\Delta_{centers} \tan(\phi)}{r_{pitch}} = \frac{(\delta) \tan(\phi)}{r_{pitch}} = 0.03mm \tag{4.5}$$

Due to the large difference in backlash between the inherent backlash in the motor and the backlash due to the gears on attached to the motor and the turntable, we can neglect the contribution to backlash from the load transmitting gears.

To ensure rail alignment at each of the required positions without over constraining the system, the backlash of the motor was included as a design parameter. The motor is able to align the turntable rails within 4° of the desired position after taking into account the backlash of the motor. To facilitate the proper alignment without causing undue stress on the motor, a spring-loaded kinematic coupling [13] was designed and can be seen in Fig. 4-3 and Fig. 4-4. When designing the kinematic coupling, it was imperative that the coupling be able to maintain its position when a carriage was traveling across the turntable as well as be able to release its position when force was applied by the turntable motor. The equations for calculating the kinematic coupling spring and pre-load requirements using the free body diagram seen in Fig. 4-3 are seen below.

$$F_{\text{preload}} = k\left(\Delta x_{\text{preload}}\right) \geq \frac{F_{\text{carriage,g}}}{3}$$
$$k \geq \frac{1.96N}{3\left(.0009m\right)} \geq 714.4\frac{N}{m} \tag{4.6}$$

$$F_p = k\left(\Delta\left(x_{\text{preload}} + x\right)\right) \leq \frac{F_{\text{motor}}}{3}$$
$$k \leq \frac{97.98N}{3\left(.0009m + .0025m\right)} k \leq 3166\frac{N}{m} \tag{4.7}$$

Based on spring availability, a spring that was 9.53 mm long and had a spring constant of 1325.7 $\frac{N}{m}$ was implemented into the kinematic coupling design.

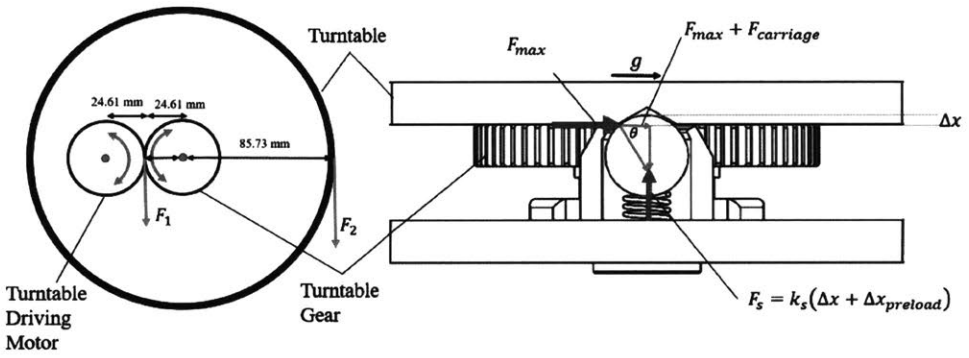

Figure 4-3: The free body diagram of the turntable kinematic coupling

To avoid Abbé errors when mounting the turntable on the wall, the wall mount, depicted in Fig. 4-5, was designed to distribute the moment of the turntable as it is acted upon by the carriages and gravity. A shoulder bolt is fed through the top of the turntable and kinematic coupling and rests on a thrust washer to ensure smooth turning. A set of radial bearings and a shaft bearing provide the necessary stabilizing force required to hold the turntable base plate parallel to the wall while bearing the weight of the carriages and cargo.

In the full assembly shown in Fig. 4-6, thirteen turntables have been constructed to implement a Vertical Hexa-Grid rail structure.

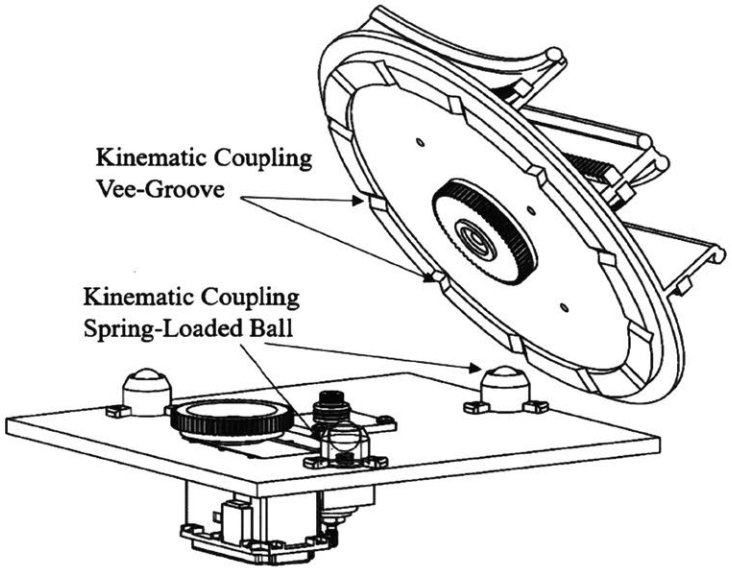

Figure 4-4: The design of the rail system and transition turntable platform

4.2 Carriage Design

4.2.1 Pinion Design

As seen in Fig. 4-7, the base of the carriage is modeled to resemble that of a roller coaster. Three sets of radial bearings act as wheels that grip the rails on three sides to constrain the carriage. To counteract the gravity load and prevent jamming, the carriage is driven by a pair of individually driven gear motors. To ensure that the carriage would be able to traverse the connection point between the MTE rail system and the turntable rails, it was necessary to design a pinion system that could account for slight misalignment of the rails as well as imperfections in the rack system. For example, if the rack teeth on the perimeter of the turntable were damaged, it is possible that the pinions driving the carriage could become stuck between the turntable rack teeth and the MTE rail teeth. Therefore, it was determined that a pair of pinions on each side of the carriage could provide the necessary driving force such that if one pinion encounters rack teeth that are damaged, the other driving pinion would compensate and allow the carriage to continue moving until both pinions were properly engaged. To avoid over constraining the carriage by having the each of

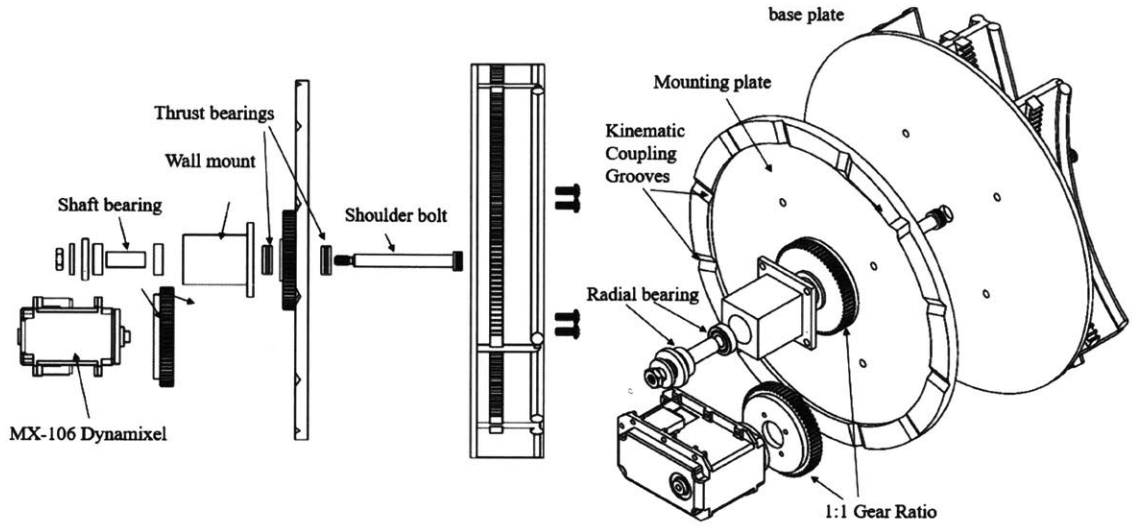

Figure 4-5: An exploded view of the turntable assembly

the four pinions independently driven, the carriage was designed such that each gear motor is attached to a single drive pinion which then powers two additional pinions on either side of the carriage. These additional two pinions on each side of the carriage are then mated to the rack teeth on the rail system.

To accommodate the additional pinions on the carriage, the length of the wheelbase of the carriage was required to be extended, however if the wheelbase was extended past a certain point, the carriage would jam when going around the curved rails. To determine the optimal length of the wheelbase, concentric circles representing the curved portions of the rails were drawn and as well as a rectangle representing the center points of the up-stop wheels on the carriage. The distance between the center of the up-stop wheels and the edge of the curved rails was measured as the wheel base was increased. It was determined that a wheelbase of 12.7 mm was the largest wheelbase that would not cause the system to jam or the wheels of the carriage to slip off the rails. This conclusion was further validated by 3D printing multiple carriages with wheelbases varying from 16.51 mm - 44.45 mm. This additional testing showed that although a carriage with a wheelbase of 12.7 mm was impeded by greater friction due to the tightness in which it interacted with the curved rails. Therefore, it was deemed that a carriage with a wheelbase of 31.75 mm provided the best com-

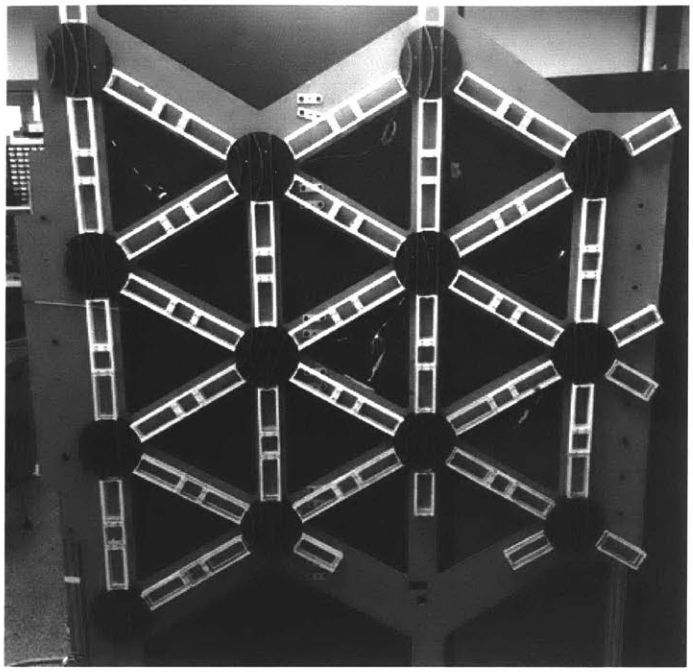

Figure 4-6: The constructed realization of the turntable and rail assembly used for testing

promise between wheelbase length and ease of motion around the curved paths. This wheelbase size allows for at least one of the drive pinions to be engaged with the rack teeth at all times, including when overcoming a potential rack teeth gap when transitioning from the turntable to the MTE rail.

The space constraints between the curved and straight rails on the turntable limits the size of the pinion that can be attached to the carriage. For this reason, the pinions were designed to have an pitch diameter of 12.7 mm, and a diametral pitch of 24.

4.2.2 Rack Design

As seen in Fig. 4-2, the turntable rails and connecting rails are fitted with rack teeth that are 6.35 mm thick and have a diametral pitch (DP) of 24 that are designed to mate with pinions on the carriages shown in Fig. 4-8. The width of the carriage was designed so that when the carriage travels along the rails, the mounting distance, A

of the pinions on the carriage are positioned using the equation below.

$$A = \frac{D_p}{2} + H = 11.69mm \tag{4.8}$$

The mounting distance for the pinions of the carriage is equal to the pitch radius, $\frac{D_p}{2}$, added to the height of the pitch line of the rack, H.

The rack teeth for the straight rail segments in the MTE rail network as well as on the turntable were adapted from the design of a standard rack. The rack teeth attached to the straight segments on the turntable were cut such that there is a seamless continuation of rack teeth during the transition between the rail network and the turntable.

To determine the location and curvature of the curved rail segments, two guide lines angled at 120° from each other. A curved line was drawn such that it was tangent to the two guide lines. To ensure the smooth transition between the MTE rail network and the turntables, the curved rails on the turntables must be in-line withe the MTE rails. This is accomplished by drawing a third guide line at each end of the curved line. This guide line is the same width as the rail segment and it is tangent to the edge of the turntable. Two more curved lines were drawn such that they follow the same path as the original curved guide line, however these lines connect the end points of the third guide line. The base of the curved rails use these two new curved lines as their guide lines. The schematic for the determination of the grid centerlines is depicted below.

The rack teeth for the outer curved rail segments on the turntable was developed by creating an large spur gear with a diametral pitch of 24 and 394 teeth. The gear was modified to contain a portion with an equal arc length to that of the curved rail and sectioned such that the first rack teeth of the curved section properly aligned with the ending rack teeth of the racks on the MTE rail network.

The rack teeth for the inner curved rail segments on the turntable was developed by creating an large involute gear with a diametral pitch of 24 and 271 teeth. The gear was modified to contain a portion with an equal arc length to that of the inner

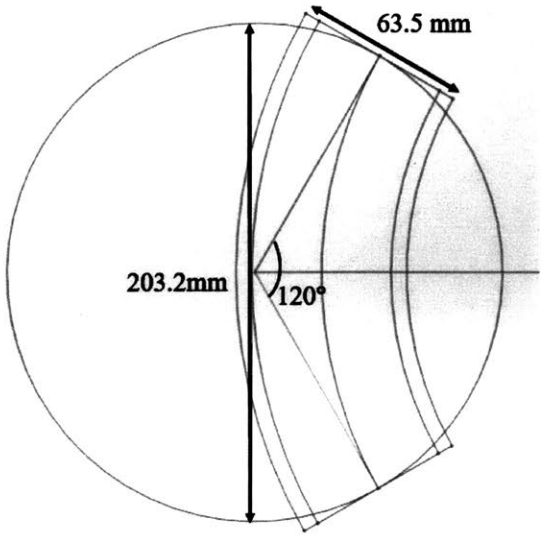

Figure 4-7: The schematic detailing the location of the curved rails on the turntables

curved rail and sectioned such that the first rack teeth of the curved section properly aligned with the ending rack teeth of the racks on the MTE rail network. Due to the curved rail sections of the turntable following a curved centerline, the arc length of the inner curved rail is exactly $\frac{2}{3}$ of the outer curved rail and contains $\frac{2}{3}$ the amount of rack teeth.

In the event of a loss of power, the gear motors will prevent system from being back-drivable and locks the carriage into place.

$$F_g = (.2kg)\left(9.8\frac{m}{s^2}\right) = 1.96N \tag{4.9}$$

$$\tau_{\text{motor}} = F_g r_{\text{pinion}} = (1.96N)\,(.003175m) = .0062Nm \tag{4.10}$$

As seen in (14.10) above, very little torque is required to move such a small mass against the force of gravity. However, by adding flexibility in the weight specification of the carriage and the desire to ensure the ability to overcome small rail misalignments, the carriage motors were chosen to have a 291:1 gear ratio and a maximum output torque of 0.5 Nm with a recommended continuous load of 0.1765 Nm. Even with a continuous load, the chosen carriage motors provide nearly thirty times the required torque to drive the carriage, thus allowing for a significant decrease in applied

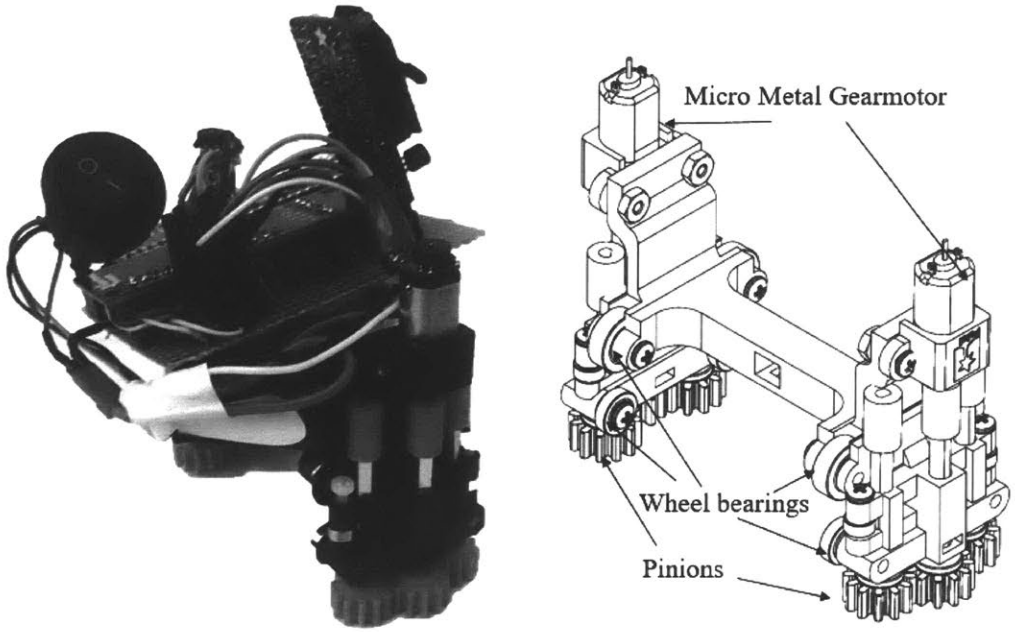

Figure 4-8: A photograph of the prototype carriage design

torque to increase the speed of the carriage with a continuous factor of safety.

$$F_{\text{motor}} = \frac{T_{\text{motor}}}{r_{\text{pinion}}} = \frac{0.1765Nm}{.003175m} = 55.6N \tag{4.11}$$

The prototype, shown in Fig. 4-8, an Arduino Micro and dual-motor driver are responsible for controlling the gearmotors. A quadrature encoder is attached to each of the motors and is used in conjunction with a PI-controller to ensure the constant velocity of each of the gearmotors.Each carriage is also equipped with a Series 1 Xbee for communication with a central controller as well as an IR receiver for receiving the localizing IR LED signals. The IR receiver is mounted in a slot along the centerline of the carriage. The IR receiver faces downward, towards the surface of the rail network, so that it may receive incoming IR LED signals.

Chapter 5

Numerical and Experimental Validation

5.1 Comparison with Current Available Elevator Systems

The design of the Vertical Hexa-Grid structure and turntable assembly was evaluated by comparing the effectiveness of this rail system to that of a Dual Standard Elevator Shaft (DSES) where two carriages share a single elevator shaft and the CME System [1]. In this context, the effectiveness of a system is defined as the normalized time required to transport cargo between two arbitrary points. The designs were also evaluated based upon the ability for carriages to transition through direction changes without stopping.

As shown in Fig. 5-1, one simple method for comparing the effectiveness of the different elevator systems is by assigning three arbitrary cargo transportation tasks to each of the systems. Assuming the travel speed and product handling time of the elevator carriages is virtually identical for the three systems, the efficiency depends on the architecture of rail network alone.

The modified DFS algorithm was applied to the MTE System and compared with the optimal route for the DSES and CME Systems, as shown in Figs. 5-1 and 5-2.

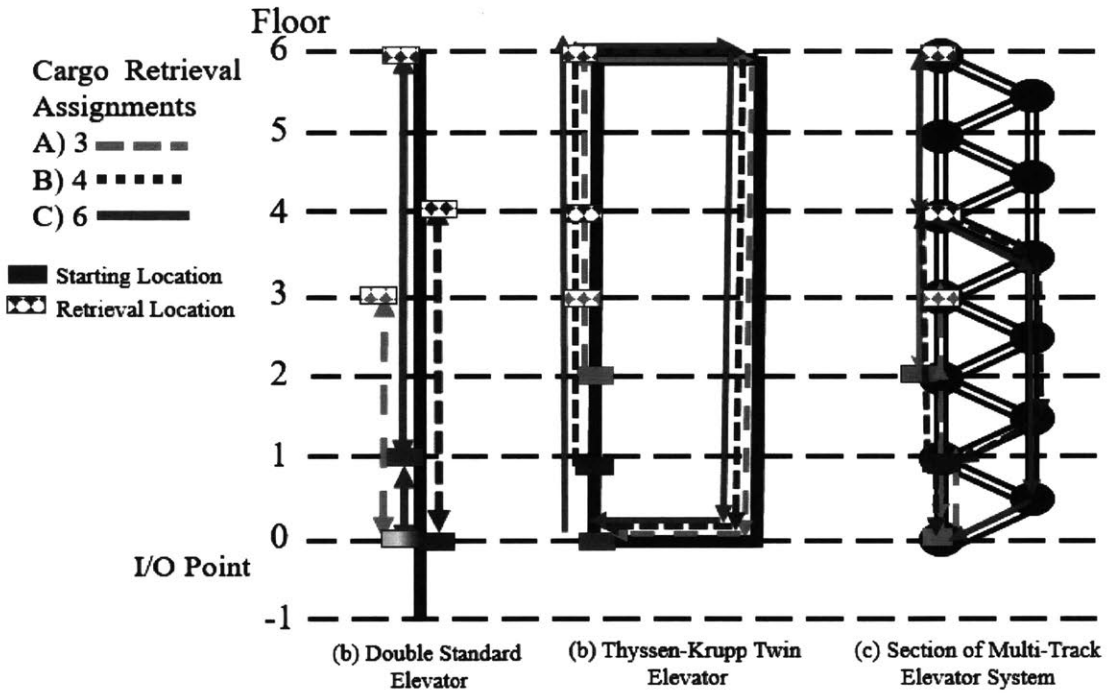

Figure 5-1: Comparison of carriage travel for (a) Dual Standard Elevator Shaft, (b) the Circular Motion Elevator system and (c) the Multi-Track Elevator System

For the three retrieval tasks the scheduling of the DSES, seen in Fig. 5-1(a), requires the coordination of the upper and lower elevators to avoid collisions from occurring. The timeline for the optimal efficiency of system for this operation can be seen in Fig. 5-2. The lower elevator reaches its destination first and begins loading the cargo as the upper elevator reaches the sixth floor. As the upper elevator is loading the cargo, the lower elevator begins its descent. As the lower elevator finishes unloading its cargo at the I/O point, and descends to the lowest level while the upper elevator approaches the I/O point. The upper elevator unloads its cargo, ascends to the the third floor to retrieve the cargo and returns to the I/O point.

The timeline for the CME system, seen in Fig. 5-1(b), is shown in Fig. 5-2. All three elevators begin to ascend and stop at their respective floors and retrieve their cargo. The middle and lower elevators are required to wait for a short period of time as the upper elevator continues the cyclical motion and begins its descent. As each elevator descends it continues horizontally to the I/O point and unloads its cargo.

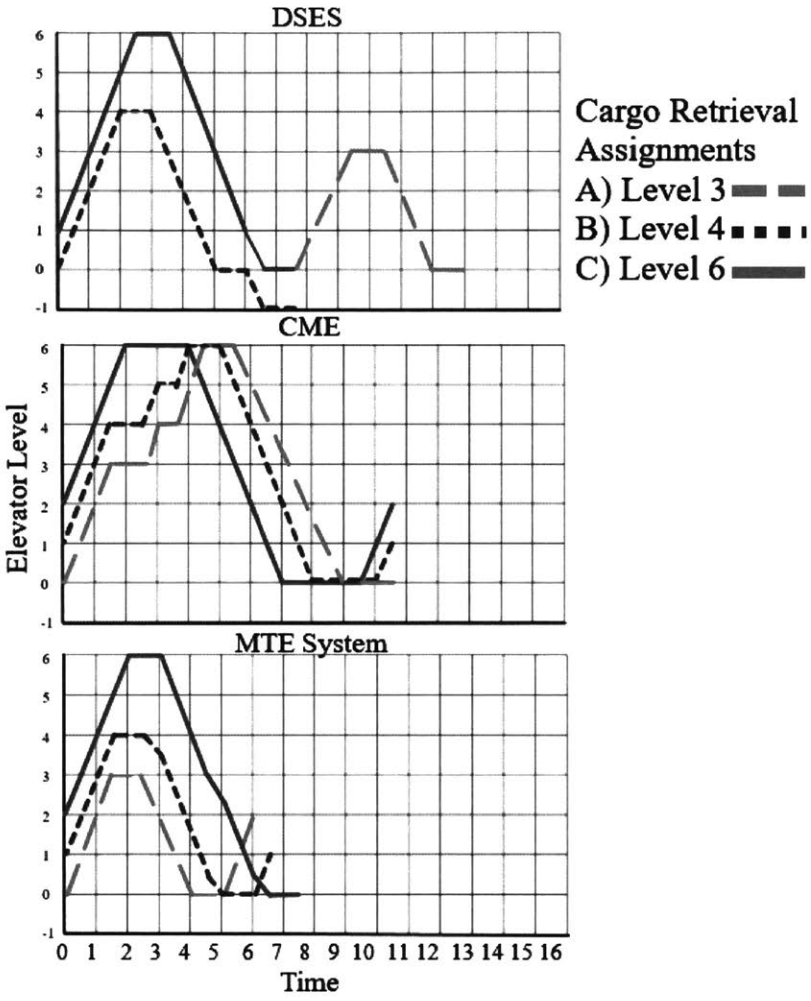

Figure 5-2: Comparison of timeline for carriage travel for a dual standard elevator shaft, the CME System and the MTE System

Using the MTE system, shown in Fig. 5-1(c), a carriage is able to pick up the cargo on the left side of the sixth floor, descend at a downward angle to the turntable on the right side of the fourth floor. When executing the second task, a carriage is able to pick up the cargo at the right turntable on the fourth floor and descend to the turntable on the left side of the second floor. Finally, to complete the third task a carriage is able to pick up the cargo at the rightmost turntable on the sixth floor and descend to the rightmost turntable on the second floor without requiring a direction change. In a full-scale realization of the Multi-Track Elevator System, the Hexa-grid rail architecture will be much more expansive and will contain many more nodes, thus

being able to complete the cargo transportation from a much wider array of cargo assignments.

As mentioned previously, our study assumes that the elevator cabins of all three systems travel at approximately the same speeds. Therefore, the effectiveness of each system is evaluated solely on architecture, without requiring a specific time scale. As seen in the cargo transportation comparison timeline depicted in Fig. 5-2 above, the effectiveness of the dual standard elevator shafts is limited by the requirement that the elevators can not cross paths. This is particularly apparent when viewing the execution of the second and third arbitrary transportation tasks. In these cases, although the lower elevator finishes its task first, it can not pass the upper elevator. The CME Elevator is more effective than the standard elevator system because it is able to transport all three cargo loads without any path interference. However, depending on the assigned task, this system still requires each elevator cabin to initially travel in a direction opposite to that of its final destination. In these instances, the multi-directionality and flexibility of the Multi-Track Elevator system allows the carriages to travel directly towards their respective final destinations while simultaneously scheduling to account for path overlapping and interference.

5.2 Collision Avoidance and Complex Maneuvers

The advantages of the Hexa-Grid structure and its application in logistics centers can be highlighted by observing the complex patterns and scheduling that can be executed. A common scenario, shown in Fig. 5-3, occurs when multiple carriages are carrying loads towards destinations that require their shortest distance paths to overlap with one another. The time-line of the complex maneuver, shown in Fig. 5-4, indicates that although not all individual carriages may not take the optimal shortest path, they are able to maintain continuous motion throughout the duration of their travel while simultaneously avoiding routing collisions. For simplicity, a simplified version of the MTE system containing 10 turntables instead of 14 is depicted.

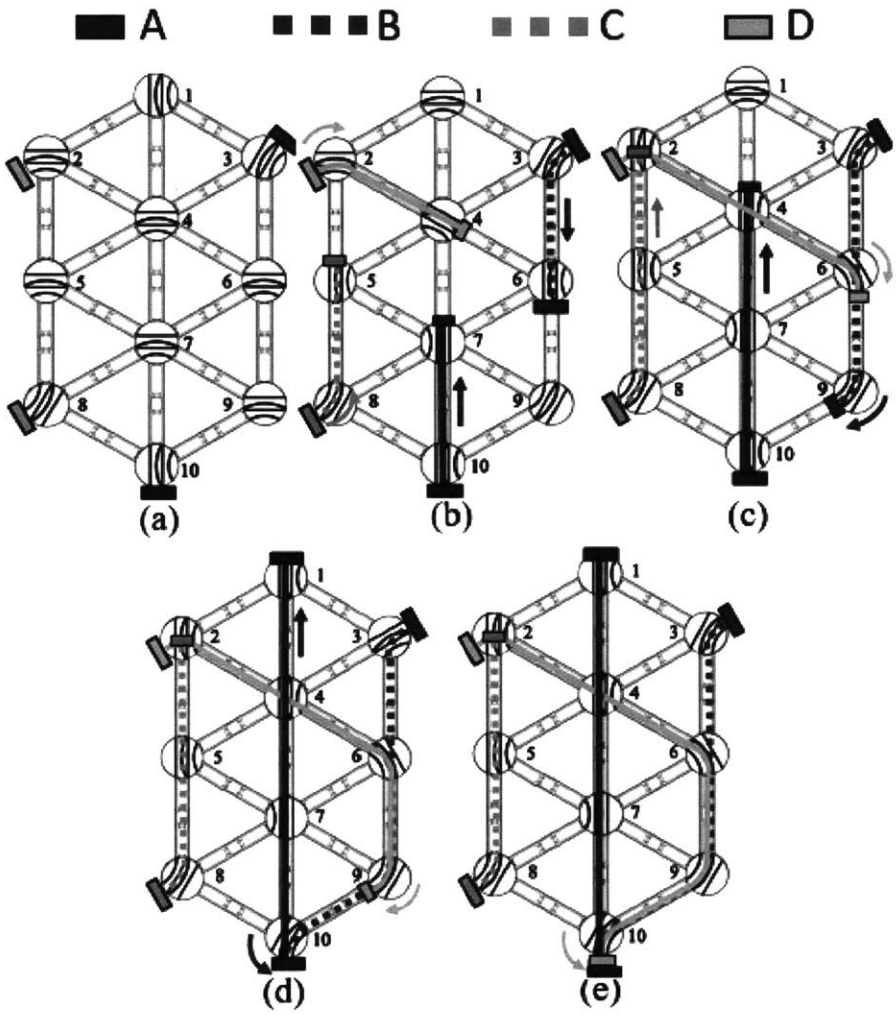

Figure 5-3: A complex pattern executed by four carriages on the Multi-Track Elevator System.

5.3 Travel Time and Total Distance Traveled

When observing a complex pattern, such as the one shown in Fig. 5-3, we can see that the individual carriages do not necessarily take the shortest possible path to reach their desired location.

A comparison can be made between the total time spent and distance traveled for situations in which a carriage is traveling the shortest distance pattern, Fig. 5-5(b) as well as the continuous motion scheduling pattern, Fig. 5-5(a).

Using the prototypes depicted in Figs. 4-6 and 4-8, the average travel time between

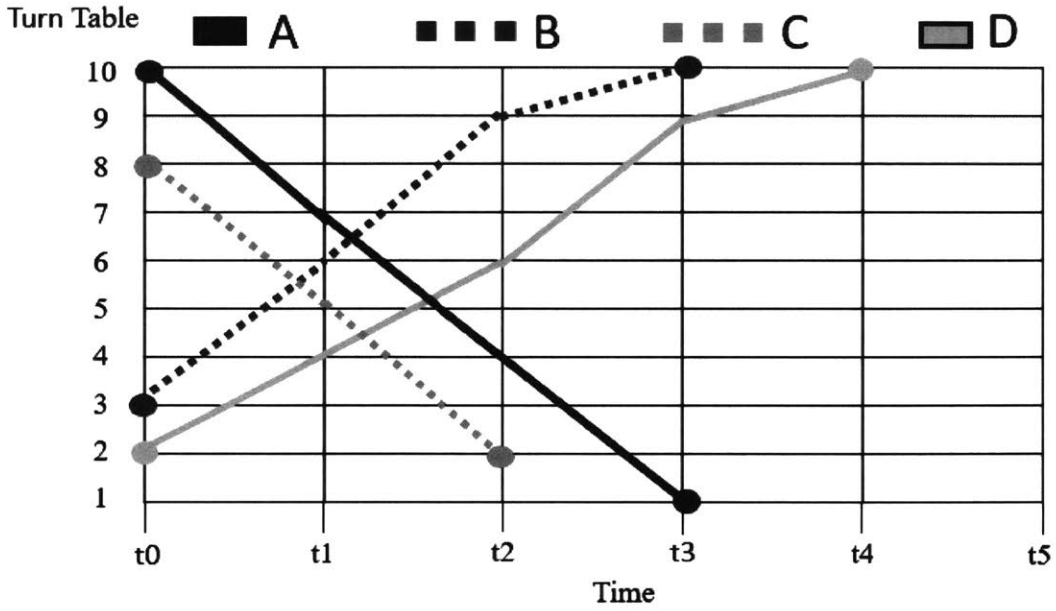

Figure 5-4: The timeline for a complex pattern executed by four carriages on the Multi-Track Elevator System.

the center of two turntables is approximately nine seconds. As shown in Table 1, the Continuous Motion Schedule (CMS) has a farther average distance traveled than the Shortest Path Traveled Schedule (SPT). However, the SPT takes 12 seconds longer to complete than the CMS. Therefore, if total travel distance is of lesser priority than total time, the Continuous Motion Schedule can be implemented. However, if the costs associated with continuous motion of the carriages are greater than those of time lost due to waiting, then the Multi-Track Elevator System carriages can be scheduled such that they take the shortest path.

The ability of carriages to take longer distance routes so that they may remain in continuous motion is critical when the optimal route of carriages with high priority tasks intersects with carriages assigned to lower priority tasks. The carriages assigned to the higher priority tasks are able to take the shortest possible path to their destination, while the carriages with less critical tasks are able to take a longer path, yet still make progress toward their destination [2].

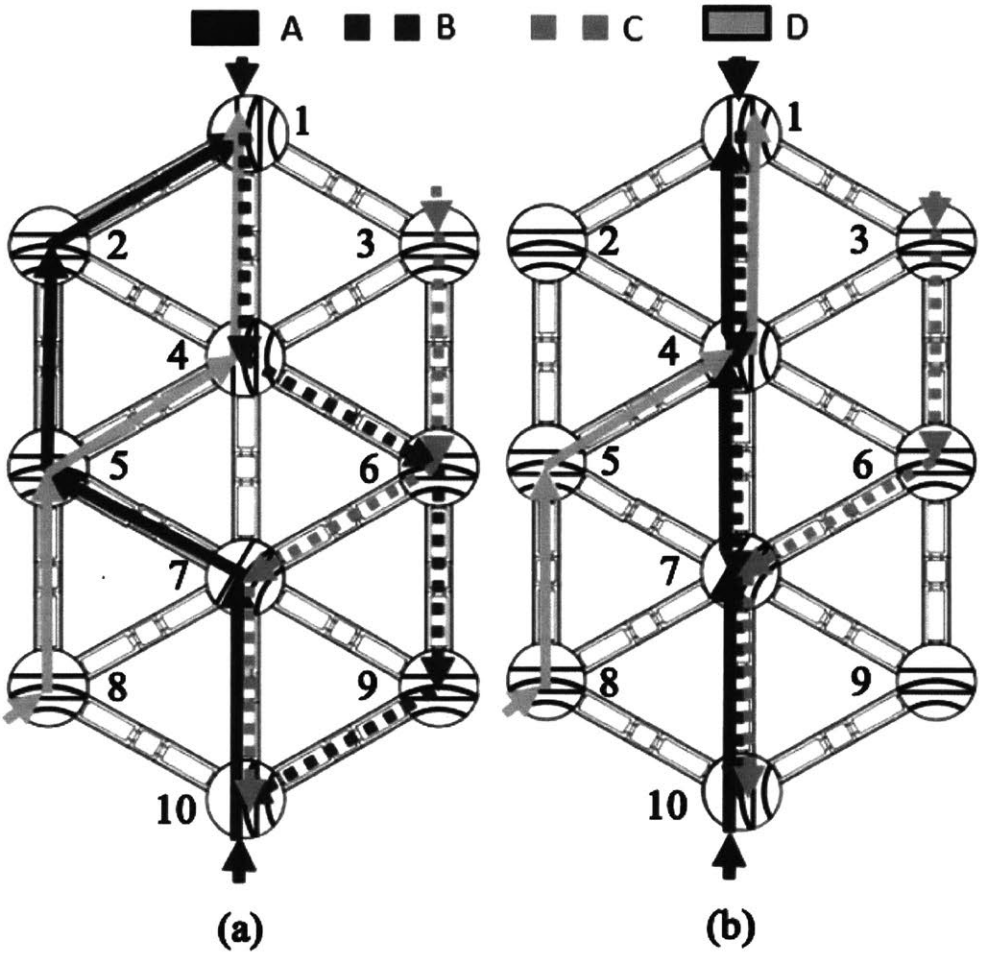

Figure 5-5: A comparison of the (a) Continuous Motion Scheduling and (b) Shortest Path Traveled Scheduling of four carriages

Table 5.1: Continuous Motion Schedule (CMS) vs. Shortest Path Traveled (SPT)

Carriage Color	A	B	C	D
Total Distance (mm) CMS	2540	2540	1956	1956
Total Distance(mm) SPT	1956	1956	1956	1956
Total Travel Time(seconds) CMS	36	36	27	27
Total Travel Time(seconds) SPT	27	27	27	27
Total Waiting Time(seconds) CMS	0	0	0	0
Total Waiting Time(seconds) SPT	27	0	9	9
Total Circuit Time(seconds) CMS	36	36	27	27
Total Circuit Time(seconds) SPT	54	27	36	36

Chapter 6

Conclusion and Future Work

6.1 Conclusion

The MTE System has promise to be a significant advancement from current elevator standards available on the market today in terms of cargo transportation efficiency and its application to the e-commerce industry. Due to the ability to avoid routing conflicts, remain in continuous motion while avoiding collisions and the bi-directionality of each of the rails, the MTE system provides each carriage with a greater freedom of route choice and execution than that of the standard elevator and the CME system. Furthermore, the MTE system allows for carriages to reach their desired location at an overall faster normalized rate than the standard elevator and CME system. If distance traveled on the MTE system is of higher priority than the total time taken to complete the assigned tasks, the MTE system is able to schedule carriage paths such that they each take the shortest distance to their end goal at the expense of sacrificing total time to complete the task. However, if the total time executing tasks is to be minimized, then the MTE system is able to execute scheduled carriage paths that are the best compromise between total distance traveled and shortest path to destination. Using this method, each carriage remains in continuous motion and are constantly making progress towards their end goals, although they may not necessarily be taking the shortest possible route towards their goals. Thus, the MTE system provides a highly adaptive scheduling capability.

6.2 Future Work

6.2.1 Optimization of Carriage Scheduling Algorithm

As previously stated, elevator path planning has been extensively studied and is an incredibly complex problem. Although developing a robust path planning algorithm was not the focus of this work, a basic path planning algorithm was created for the purposes of testing the MTE system. The algorithm, described in chapter 3, calculates the shortest path for multiple carriages such that they do not collide, nor do they have to stop moving. In reality, it is entirely possible that the true optimal path may contain a combination of the continuous motion scheduling and the shortest path scheduling. For example, a threshold may be determined for which waiting for a turntable to be available reduces the overall system time. An example of implementing this threshold continuous motion (TCM) can be seen in the figure and table below.

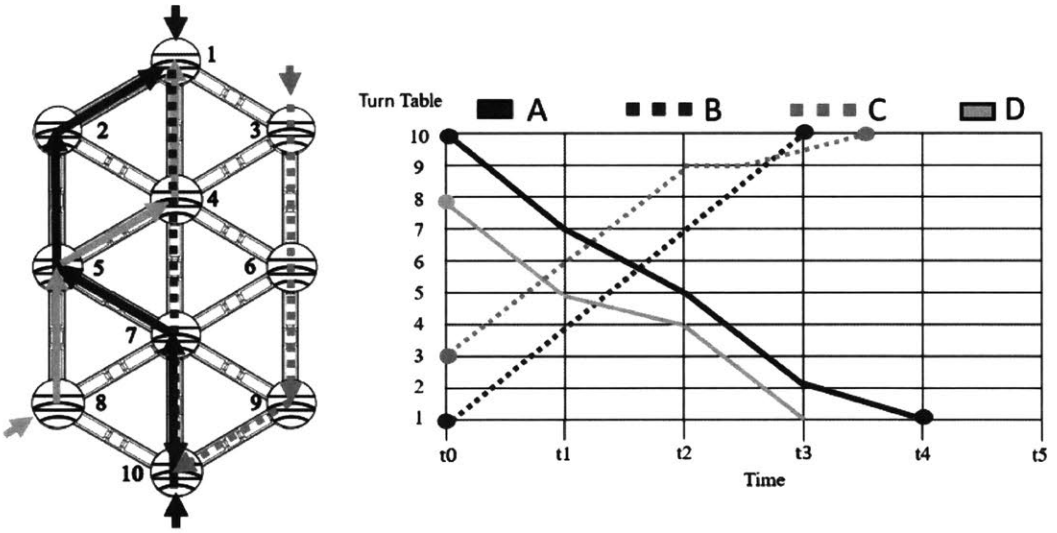

Figure 6-1: The path and timing of the MTE system using a threshold to determine waiting for an available turntable

It can be seen from the table above that the TCM scheduling reduces the total circuit time for the entire system. Further investigations will be made into optimizing the TCM scheduling algorithm to find the optimal waiting time threshold as well as optimizing the cost function of traveling along each rail segment to produce more

Table 6.1: The total distance and time for the TCM scheduling

Carriage Color	A	B	C	D
Total Distance (mm) TCM	2540	1956	1956	1956
Total Travel Time(seconds) TCM	36	27	27	27
Total Waiting Time(seconds) TCM	0	0	4.5	0
Total Circuit Time(seconds) TCM	36	27	31.5	27

optimal system paths.

6.2.2 Implementation of Horizontal Transition of Carriages

In order to integrate the MTE system with current warehouse automation technology, such as the AVS/RS or SBS/RS systems, a mechanism by which the MTE carriages are able to enter the horizontal plane must be developed and tested. One such strategy is depicted in figure 6-2 below.

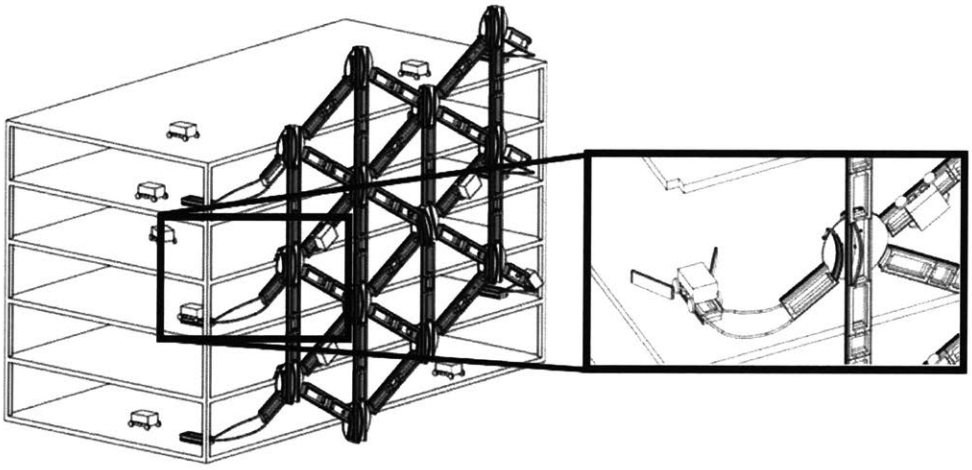

Figure 6-2: The implementation of a helical rail in the MTE System

As seen in figure 6-2, implementing a helical rail may allow for the carriages to transition to the horizontal plane. If the carriages are able to travel between the storage isles of products, as in the SBS/RS system, it would eliminate the need for a second product-transporting shuttle. This could potentially reduce product transportation time and increase productivity of the entire warehouse.

Bibliography

[1] Thyssenkrupp premieres multi, worlds first rope-less elevator system-first scale model launched with four cabins in loop operation.

[2] Maren Bennewitz, Wolfram Burgard, and Sebastian Thrun. Optimizing schedules for prioritized path planning of multi-robot systems.

[3] Peter Brass, Flavio Cabrera-Mora, Andrea Gasparri, and Jizhong Xiao. Multirobot tree and graph exploration.

[4] Richard G. Budynas, Joseph Edward Shigley, and J. K. Nisbett. *Shigley's Mechanical Engineering Design.*

[5] Hector J. Carlo and Iris F. A. Vis. Sequencing dynamic storage systems with multiple lifts and shuttles.

[6] Loretta Chao. Room to grow: Warehouses super-size to meet e-commerce demands.

[7] E.W. Dijkstra. A note on two problems in connexion with graphs.

[8] Jean-Claude Latombe. *Robot Motion Planning.* Springer, 1991.

[9] Tone Lerher. Simulation analysis of shuttle based storage and retrieval systems.

[10] Charles J. Malmborg. Conceptualizing tools for autonomous vehicle storage and retrieval systems.

[11] Charles J. Malmborg. Interleaving dynamics in autonomous vehicle storage and retrieval systems.

[12] Gino Marchet, Marco Melacini, Sara Perotti, and Elena Tappia. Analytical model to estimate performances of autonomous vehicle storage and retrieval systems for product totes.

[13] Alexander H. Slocum. *FUNdaMENTALS of Design.*

[14] Marc Wulfraat. Is kiva systems a good fit for your distribution center? an unbiased distribution consultant evaluation. *MWPVL International White Papers*, 2012.

[15] Peter R. Wurman, Raffaello D'Andrea, and Mick Mountz. Coordinating hundreds of cooperative, autonomous vehicles in warehouses. pages 1752–1759, 2007.

[16] Xue Yinghua and Liu Hongpeng. Intelligent storage and retrieval systems based on rfid and vision in automated warehouse.